Characterization of homogeneous recombinant rat ovarian 20α-hydroxysteroid dehydrogenase: fluorescent properties and inhibition profile

Haiching MA and Trevor M. PENNING[1]

Department of Pharmacology, University of Pennsylvania School of Medicine, 3620 Hamilton Walk, Philadelphia, PA 19104, U.S.A.

In rat ovary, 20α-hydroxysteroid dehydrogenase (20α-HSD), a member of the aldo-keto reductase (AKR) superfamily, converts progesterone into the inactive progestin 20α-hydroxyprogesterone and has been implicated in the termination of pregnancy. Here we report a convenient overexpression system that permits the purification of milligram quantities of homogeneous recombinant 20α-HSD with wild-type enzyme activity. The availability of this enzyme has permitted detailed kinetic, inhibition and fluorescence analyses. The enzyme exhibited narrow steroid specificity, catalysing reactions only at C-20; it reduced progesterone and 17α-hydroxyprogesterone and oxidized 20α-hydroxypregnanes. It also turned over common AKR substrates, such as 9,10-phenanthrenequinone and 4-nitrobenzaldehyde. The intrinsic fluorescence spectrum of 20α-HSD was characterized and was quenched on the binding of NADP(H), yielding a K_d^{NADP} of 0.36 μM and a K_d^{NADPH} of 0.64 μM. NADP(H) binding generated an energy transfer band that could not be quenched by steroids. Inhibition studies conducted with non-steroidal and steroidal anti-inflammatory drugs and synthetic oestrogens indicated that even though rat ovarian 20α-HSD and rat liver 3α-hydroxysteroid dehydrogenase (3α-HSD) share more than 67% amino acid identity, their inhibition profiles are markedly different. Unlike 3α-HSD, most of these compounds did not inhibit 20α-HSD. Only meclofenamic acid and hexoestrol were potent competitive inhibitors for 20α-HSD, yielding K_i values of 18.9 and 14.3 μM respectively. These studies suggest that selective non-steroidal AKR inhibitors could be developed for 20α-HSD that might be useful in maintaining pregnancy and that specific inhibitors might be developed from either *N*-phenylanthranilates or biphenols.

Key words: aldo-keto reductase, *N*-phenylanthranilates, pregnancy, progesterone, synthetic oestrogens.

INTRODUCTION

Rat ovarian 20α-hydroxysteroid dehydrogenase (20α-HSD) converts progesterone to the biologically inactive steroid 20α-hydroxyprogesterone (20α-OHP), with NADPH as cofactor [1,2]. In pregnant rats, the induction of 20α-HSD activity in the corpus luteum and the subsequent increase in circulating 20α-OHP levels precedes parturition [3]. During labour, human placental 20α-HSD activity increases and this is accompanied by a decrease in the ratio of progesterone to 20α-OHP [4,5]. These observations indicate an important role for 20α-HSD in terminating pregnancy. 20α-HSD is also important in regulating cell growth; enzyme inhibition strongly attenuates cell growth in a canine osteosarcoma cell line [6]. In postmenopausal women, hormone-dependent breast cancer responds best to hormonal ablative therapy provided that the tumours are positive for both oestrogen and progestin receptors [7]. Although oestrogen is the dominant mitogenic hormone required for tumour growth, progesterone can provide a synergistic effect. As a consequence, 20α-HSD isoforms might have important roles in regulating the intracellular concentration of progesterone; depending on whether they act as reductases or dehydrogenases they could either blunt or abrogate the tumour response to oestrogen [7,8].

The rat ovarian 20α-HSD cDNA and its corresponding gene have been cloned [9–11]. The deduced amino acid sequence is more than 60% identical with rat liver 3α-hydroxysteroid dehydrogenase (3α-HSD), the human 3α-HSD isoforms and mouse liver 17β-HSD, which are all members of the aldo-keto reductase (AKR) superfamily [12,13]. Because of the limited availability of rat ovarian 20α-HSD [14,15], its detailed characterization including kinetic, inhibition, fluorescence and crystallographic studies has lagged behind those of other AKRs. Previous attempts have been made to purify and characterize the recombinant enzyme expressed in *Escherichia coli* and baculovirus-infected insect cells, but this has led to an enzyme of low activity relative to the wild type and these recombinant forms have had limited utility [16].

In the present study we established an overexpression system that allows the purification of large quantities of highly active recombinant 20α-HSD by conventional chromatographic methods. The purified protein has a specific activity comparable to that of native protein with progesterone and 20α-OHP as substrates [14]. Kinetic, spectral and inhibitory properties of the recombinant enzyme are described. Because its inhibition profile is markedly different from that of rat liver 3α-HSD, these studies suggest that selective non-steroidal inhibitors could be developed to modulate 20α-HSD activity to maintain pregnancy.

MATERIALS AND METHODS

Materials

Trizol® reagent and Superscript™ reverse transcriptase were purchased from Life Technologies. Vector pCR™ II was obtained from InVitrogen Corporation; the vector pET16b was purchased from Novagen. XL1-Blue supercompetent cells were obtained from Stratagene. pET–20α-HSD was expressed in *E. coli* strain C41 (DE3), which was kindly provided by Dr. J. E. Walker (MRC Laboratory of Molecular Biology, Cambridge,

Abbreviations used: AKR, aldo-keto reductase; ARIs, aldose reductase inhibitors; $C_{20\text{-}17}$-lyase, 17α-hydroxylase-17,20-lyase (also $P450_{17\alpha}$ or CYP17); 3α-HSD, 3α-hydroxysteroid dehydrogenase (EC 1.1.1.213, A-face-specific, now also designated AKR1C9); 20α-HSD, 20α-hydroxysteroid dehydrogenase (EC 1.1.1.149, now also designated AKR1C8); IPTG, isopropyl β-D-thiogalactoside; βME, 2-mercaptoethanol; NSAIDs, non-steroidal anti-inflammatory drugs; SAIDs, steroidal anti-inflammatory drugs; 20α-OHP, 20α-hydroxyprogesterone.

[1] To whom correspondence should be addressed (e-mail penning@pharm.med.upenn.edu).

U.K.). The primers used for PCR-based cloning were synthesized by Gibco BRL. All restriction enzymes were purchased from New England Biolabs. NAD(H) and NADP(H) were from Boehringer-Mannheim. All steroids were obtained from Steraloids. [4-^{14}C]Progesterone (50 mCi/mmol) was from NEN-DuPont. Whatman DE-52 was from Baxter, Red-Sepharose was from Pharmacia Biotech, and Dyematrex Gel Green A and Centriplus® 10 concentrators were purchased from Amicon. All other compounds were of ACS grade or better and obtained from Sigma-Aldrich.

Cloning rat ovarian 20α-HSD

On the basis of the published cDNA sequence of 20α-HSD [9,10], we designed two PCR primers. The forward primer contained an *Nco*I site upstream from the initiation codon, 5′-GGGCCATGGATTCCAAAATTCAGAAGATGG-3′, and the reverse primer contained a *Bam*HI site downstream from the termination codon, 5′-CCCGGATCCAGGAGCTTCGAGCAGAACAC-3′, in which the underlined nucleotides indicate the restriction sites. Ovaries were removed from a 2-week-old female Sprague–Dawley rat; the total RNA was isolated with Trizol reagent by following the manufacturer's protocol. 20α-HSD cDNA was synthesized with the RNA as template by adding Superscript reverse transcriptase, the reverse primer and dNTP, and incubating at 45 °C for 1 h. The 20α-HSD cDNA was then amplified by 30 cycles of PCR with the two primers described. Each cycle had an annealing step (60 s at 55 °C), a chain extension step (120 s at 72 °C) and a denaturation step (60 s at 90 °C). The PCR product was first ligated into the PCR cloning vector pCR II and the desired cDNA fragment was released and subcloned into the expression vector pET16b. The fidelity of the cloned 20α-HSD cDNA was confirmed by dideoxy sequencing.

Expression and purification of recombinant 20α-HSD cDNA

Step 1: bacterial culture

The pET–20α-HSD vector was introduced into the C41 (DE3) cells by electroporation. For large-scale protein purification, 2 litres or more of C41 (DE3) cells containing pET–20α-HSD were grown in Luria–Bertani medium at 37 °C with 100 μg/ml ampicillin. After the A_{600} had reached 0.6, isopropyl β-D-thiogalactoside (IPTG) was added to a final concentration of 1 mM to induce protein expression overnight. The final culture was centrifuged (10000 ***g*** for 10 min), the pellets were washed with 10 mM Tris/HCl buffer, pH 8.6, containing 1 mM EDTA and 1 mM 2-mercaptoethanol (βME), then harvested by re-centrifugation. The final pellets were resuspended in the same buffer and lysed by sonication with a Fisher Scientific 500 Sonic Dismembrator. The sonicate was pooled after centrifugation (16000 ***g*** for 30 min) and dialysed overnight against 10 mM Tris/HCl buffer, pH 8.6, containing 1 mM EDTA, 1 mM βME and 20 % (v/v) glycerol.

Step 2: DE-52 cellulose chromatography

The dialysed fraction was applied to a DE-52 cellulose anion-exchange column equilibrated with the dialysis buffer; the column was washed with the same buffer. Retained protein was eluted with a linear salt gradient of 0–500 mM NaCl. The peak fractions were identified by monitoring the NADP$^+$-dependent oxidation of 20α-OHP and by measuring protein content with SDS/PAGE. The peak fractions were pooled and concentrated with Centriplus 10 concentrators. The protein was dialysed overnight against 10 mM potassium phosphate buffer, pH 7.0, containing 1 mM EDTA, 1 mM βME and 20 % (v/v) glycerol.

Step 3: Dyematrex Gel Green A chromatography

The dialysed protein was applied to a Green A affinity column that had been equilibrated in dialysis buffer. The column was washed and the retained protein was eluted with a linear salt gradient of 0–2 M KCl. The peak fractions were identified as before, then pooled, concentrated and dialysed overnight against 10 mM potassium phosphate buffer, pH 7.0, containing 1 mM EDTA, 1 mM βME and 20 % (v/v) glycerol.

Step 4: Red-Sepharose chromatography

The concentrated protein was further purified on a Red-Sepharose affinity column under the same conditions as described for step 3. The peak fractions were pooled and dialysed overnight against 20 mM potassium phosphate buffer, pH 7.0, containing 1 mM EDTA, 1 mM βME and 30 % (v/v) glycerol. The homogeneous enzyme had a final specific activity of 2.1 μmol of 20α-OHP oxidized/min per mg of protein and was stored at a concentration of 2.8 mg/ml at −70 °C. Protein concentration was determined by the method of Lowry with BSA (from New England Biolabs) as standard [17].

Identification of the product of the 20α-HSD reaction

The reduction of progesterone was monitored in systems (100 μl) containing 35 μM [4-^{14}C]progesterone (40000 c.p.m.) in 4 % (v/v) acetonitrile, 200 μM NADPH and 100 mM potassium phosphate buffer, pH 6.0. All reactions were performed at both 37 and 25 °C; at various time points an aliquot was removed to confirm the identity of the product. The steroids were extracted twice with water-saturated ethyl acetate (0.4 ml each); the extracts were pooled, vacuum-dried and redissolved in 20 μl of methanol. The radioactive steroid was applied to a 20 cm × 20 cm TLC plate (Whatman) and developed in hexane/chloroform/ethyl acetate (2:2:1, by vol.). The product was identified by chromatography with authentic unlabelled 20α-OHP, which was detected by charring after being sprayed with methanol/H_2SO_4 (1:1, v/v).

Measurement of steady-state kinetic parameters

Oxidation reactions were performed in 1 ml systems containing 40 μM 20α-OHP in 4 % (v/v) acetonitrile, 200 μM NADP$^+$ and 100 mM Hepes buffer, pH 7.8, at 37 °C [14]. In the reduction direction, reactions were performed in 1 ml systems containing 35 μM progesterone in 4 % (v/v) acetonitrile, 200 μM NADPH and 100 mM potassium phosphate buffer, pH 6.0, at 37 °C. Initial velocities were measured in a Beckman DU-640 spectrophotometer by observing the rate of change of absorbance of pyridine nucleotide at 340 nm (ϵ 6270 $M^{-1}\cdot cm^{-1}$) in the 1 ml system with a 1 cm light path. Reactions were initiated by the addition of enzyme. Estimates of K_m and k_{cat} for 20α-OHP were made at 200 μM NADP$^+$, with varied steroid concentration (2.0–40.0 μM). K_m and k_{cat} values for NADP$^+$ were determined at 40 μM 20α-OHP by varying the NADP$^+$ concentration (0.5–15 μM). Kinetic constants for progesterone reduction were measured at 200 μM NADPH with varied steroid concentration (1.5–35 μM). Determination of the kinetic constants for NADPH oxidation used 35 μM progesterone and were made by varying the NADPH concentration (1–20 μM). Calculation of k_{cat} and K_m values used the ENZFITTER non-linear regression analysis program to fit untransformed data to a hyperbolic function [18,19], yielding estimates of the kinetic constants and their associated S.E.M. values. The kinetic constants of other steroid and aldose reductase substrates were determined under similar

conditions except that the reactions were conducted at 25 °C; the substrate concentrations used are listed in the appropriate tables.

Determination of K_d values for NADP(H) by fluorescence titration

Measurement of the K_d values for the binding of NADP(H) to recombinant enzyme were made by measuring protein fluorescence emission on a Perkin-Elmer Model 650-10S fluorescence spectrometer after the incremental addition of NAD(P)H (50 nM–4.0 μM). Each 1 ml sample contained 0.5 μM protein in 100 mM Hepes buffer, pH 7.8, for $NADP^+$, or 100 mM potassium phosphate buffer, pH 6.0, for NADPH at 25 °C. The total volume change due to the addition of cofactors was less than 2%. The samples were excited at 290 nm and the fluorescence emission was scanned from 300 to 500 nm at 120 nm/min with the excitation and emission bandpasses each set to 5 nm. Untransformed fluorescence data were plotted as the percentage change in fluorescence at emission λ_{max} against cofactor concentration (ΔF). These data were fitted to a saturation absorption isotherm by ENZFITTER, which provided an estimate of the K_d and the associated S.E.M. [19].

Determination of K_i values for enzyme inhibitors

The concentration of inhibitor was varied in the standard enzyme assay for measuring the oxidation of 20α-OHP to yield a family of lines. The K_i was derived from these lines by using Lineweaver–Burk plots [20]. In these reactions, the 20α-OHP concentration was varied from 0 to 35 μM; 100 mM potassium phosphate buffer, pH 7.0, was substituted for 100 mM Hepes because the latter formed chromophores in the presence of the inhibitors.

RESULTS

Expression and purification of recombinant 20α-HSD

Rat ovarian 20α-HSD was overexpressed and purified from *E. coli* C41 (DE3) cells after induction by IPTG (Figure 1 and Table 1). The final specific activity of the homogeneous recombinant

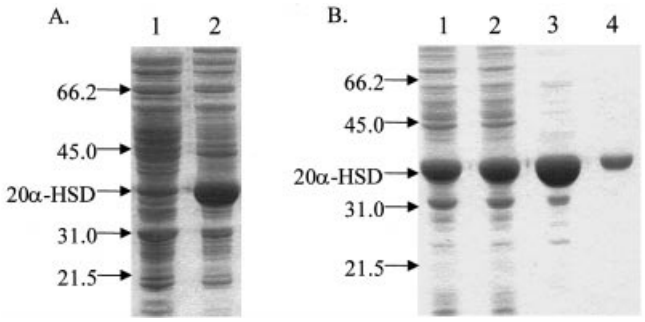

Figure 1 SDS/PAGE analysis of the induction and purification of recombinant 20α-HSD from *E. coli* strain C41 (DE3) transformed with pET–20α-HSD

(**A**) Induction with IPTG increased protein expression. Lane 1, 40 μg of bacterial cell lysate without IPTG induction; lane 2, 40 μg of bacterial cell lysate with induction by 1 mM IPTG. (**B**) Purification of recombinant 20α-HSD by conventional chromatography. Lane 1, 25 μg of bacteria cell lysate; lane 2, 25 μg of the peak fractions from DE52 cellulose column chromatography; lane 3, 15 μg of the peak fractions from Green A column chromatography; lane 4, 2.5 μg of the peak fractions from Red Sepharose column chromatography. The gel was stained with 0.2% Coomassie Blue. Arrows indicate the positions of molecular mass markers (in kDa) and the position of recombinant 20α-HSD.

Table 2 Kinetic constants of homogeneous recombinant rat ovarian 20α-HSD for its endogenous substrates

All assays were performed in a 1 ml system at 37 °C; rates were determined by measuring the change in absorbance of the pyridine nucleotide at 340 nm (see the Materials and methods section).

Substrate	k_{cat} (min^{-1})	K_m (μM)	k_{cat}/K_m ($min^{-1} \cdot \mu M^{-1}$)
20α-OHP	70 ± 0.2	9 ± 0.1	8
$NADP^+$	91 ± 6.1	8 ± 1.1	11
Progesterone	99 ± 6.7	11 ± 1.7	9
NADPH	86 ± 1.3	14 ± 4.0	6

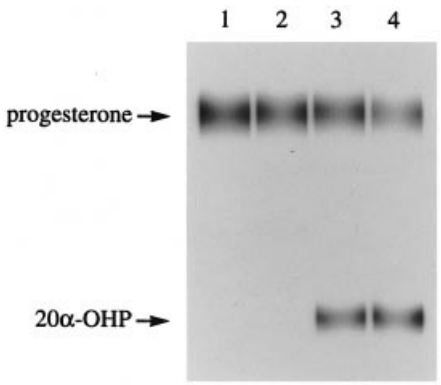

Figure 2 Identification of 20α-OHP as the product of the reaction catalysed by recombinant 20α-HSD

Lanes 1 and 2, 2 μg of recombinant 3α-HSD was incubated with 2.3 μM NADPH and 35 μM [^{14}C]progesterone for 5 min (lane 1) and 10 min (lane 2); lanes 3 and 4, conditions were the same as in lanes 1 and 2 except that 1 μg of recombinant 20α-HSD was used. The radioactive product was identified by co-chromatography with authentic unlabelled 20α-OHP.

Table 1 Purification table for recombinant rat ovarian 20α-HSD

pET-20α-HSD was expressed in *E. coli* strain C41 (DE3). All activity measurements were performed under standard assay conditions (see the the Materials and methods section).

Fraction	Total volume (ml)	Total activity (μmol/min)	Total protein (mg)	Specific activity (μmol/min per mg)	Purification factor (fold)	Yield (%)
Sonicate	22	84.4	469.0	0.18	1	100
DE52 cellulose	30	82.7	201.6	0.41	2.3	98
Green A	30	53.5	66.0	0.81	4.5	63
Red-Sepharose	3.9	23.0	11.0	2.09	11.6	27

Table 3 Kinetic constants of 20α-HSD for endogenous steroids and aldose reductase substrates

All assays were performed under the same conditions as described in Table 2 but at 25 °C. Abbreviation: CNS, central nervous system.

Substrate	Cofactor	k_{cat} (min^{-1})	K_m (μM)	k_{cat}/K_m ($min^{-1} \cdot \mu M^{-1}$)
20α-OH-5α-pregnan-3-one (CNS steroid)	$NADP^+$	47.1 ± 4.3	13.8 ± 3.5	3.4
3α-OH-5α-pregnan-20-one (CNS steroid)	NADPH	12.5 ± 1.6	12.0 ± 3.5	1.0
17α-OH-progesterone (C_{20-17}-lyase substrate)	NADPH	10.7 ± 0.8	15.4 ± 2.9	0.7
9,10-Phenanthrenequinone	NADPH	462.1 ± 26.9	1.95 ± 0.4	237.0
4-Nitrobenzaldehyde	NADPH	354.7 ± 33.4	381.1 ± 60.5	0.9
D,L-Glyceraldehyde	NADPH	12.9 ± 0.3	120000	0.00011

Table 4 Substrate specificity of recombinant 20α-HSD

All assays were performed under standard reaction conditions but at 25 °C. The concentrations used for these reactions were close to the limit of solubility. Abbreviation: n.d., not detectable by the spectrophotometer assays (less than 1 nmol/min per mg).

Substrate	Concentration (μM)	Cofactor	Specific activity (μmol/min per mg)	Site modified
5α-Pregnane-3,20-dione	60	NADPH	0.9	C-20 ketone
20α-OH-5β-pregnan-3-one	60	$NADP^+$	2.5	20α-Hydroxy group
Prednisone	30	NADPH	0.025	C-20 ketone
Prednisolone	30	NADPH	0.016	C-20 ketone
Pregnenolone	50	NADPH	0.067	C-20 ketone
17α-OH-Pregnenolone	30	NADPH	0.007	C-20 ketone
20β-OH-Pregn-4-en-3-one	50	$NADP^+$	n.d.	20β-Hydroxy group
Androsterone	75	$NADP^+$	n.d.	3α-Hydroxy group
Testosterone	50	$NADP^+$	n.d.	17β-Hydroxy group
17β-Oestradiol	50	$NADP^+$	n.d.	17β-Hydroxy group
17α-Oestradiol	50	$NADP^+$	n.d.	17α-Hydroxy group
Oestrone	50	NADPH	n.d.	C-17 ketone
5α-Dihydrotestosterone	50	$NADP^+$	n.d.	17β-Hydroxy group
	50	NADPH	n.d.	C-3 ketone
Prostaglandin E_2	60	NADPH	0.002	
D-Galactose	100000	NADPH	0.017	
D-Glucose	100000	NADPH	0.013	

protein was 2.1 μmol/min per mg, identical with that previously reported for the native enzyme purified from rat ovary with NADP(H) as cofactor [14]. The recombinant enzyme was considered homogeneous because it gave a single band of 37 kDa on SDS/PAGE (Figure 1). It was found that the DE52 cellulose chromatography step was crucial for separating large amounts of undesired protein from 20α-HSD. However, the fold purification achieved at this step was not high because 20α-HSD did not bind tightly to this anion-exchange resin. In developing the purification it was found that both Dyematrex Gel Green A and Red-Sepharose worked well in tandem as affinity steps, but neither alone gave pure protein.

Nucleotide and substrate specificity

20α-HSD is an oxidoreductase that interconverts progesterone and 20α-OHP by using NADP(H) as cofactor. Kinetic parameters are given in Table 2; product identification was verified by radiochromatography, as shown in Figure 2. However, unlike 3α-HSD in the AKR superfamily, it does not use NAD(H) as cofactor even though they share the same cofactor-binding residues [12]. 20α-HSD gave the highest catalytic efficiency with its natural substrates. The catalytic efficiencies for progesterone and 20α-OHP were 9 and 8 $min^{-1} \cdot \mu M^{-1}$ respectively (Table 2). By employing steroids containing only one reactive group (ketone or alcohol) it was found that this enzyme catalysed only reactions at the C-20 position. There was no detectable 3α, 17β or 20β activity in the preparation (Tables 3 and 4). 20α-HSD also exhibited a high activity for neuroactive steroids such as 3α-hydroxy-5α-pregnan-20-one (catalytic efficiency 1.0 $min^{-1} \cdot \mu M^{-1}$), 20α-hydroxy-5α-pregnan-3-one (catalytic efficiency 3.4 $min^{-1} \cdot \mu M^{-1}$) and 5α-pregnane-3,20-dione (catalytic efficiency 0.9 $min^{-1} \cdot \mu M^{-1}$) (Tables 3 and 4). 20α-HSD also gave a high catalytic efficiency for 17α-hydroxyprogesterone (0.7 $min^{-1} \cdot \mu M^{-1}$), a substrate of 17α-hydroxylase-17,20-lyase (C_{20-17}-lyase), but had very low activity towards another substrate for C_{20-17}-lyase, 17α-hydroxypregnenolone (for which only a specific activity of 7 nmol/min per mg could be calculated). Like other HSDs in the AKR superfamily, 20α-HSD exhibited high catalytic efficiency towards common aldose reductase substrates, e.g. 9,10-phenanthrenequinone and 4-nitrobenzaldehyde, but its catalytic efficiency for D,L-glyceraldehyde was very low and its activity with six-carbon sugars was barely detectable (Tables 3 and 4). 20α-HSD can also reduce prostaglandin E_2 at a rate comparable to those of 3α-HSD [21] and prostaglandin-E_2-9-keto-reductase [22].

Fluorescence spectra of 20α-HSD and its complexes

The intrinsic fluorescence emission spectra of apo-20α-HSD, apo-3α-HSD and their binary complexes (E · NADPH) are shown in Figures 3(A) and 3(B). 20α-HSD gave an intrinsic fluorescence

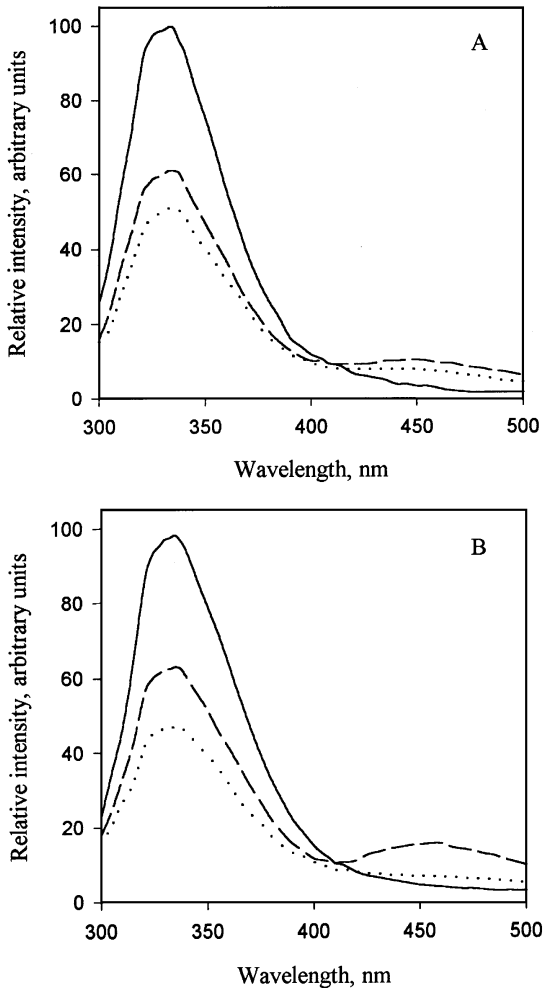

Figure 3 Fluorescence emission spectra of apo-20α-HSD and apo-3α-HSD and of their binary complexes (E · NADPH), and the effects of steroids

(**A**) Solid line, emission spectrum of 0.85 μM recombinant 20α-HSD excited at 290 nm; broken line, emission spectrum of the binary complex after the addition of 4 μM NADPH; dotted line, emission spectrum after the addition of 40 μM 20α-OHP to the E · NADPH complex. (**B**) Solid line, emission spectrum of 0.5 μM recombinant 3α-HSD excited at 290 nm; broken line, emission spectrum of binary complex after the addition of 2 μM NADPH; dotted line, emission spectrum of ternary complex after the addition of 50 μM testosterone to the E · NADPH complex. Recombinant 3α-HSD was purified as described [37].

emission spectrum with a λ_{max} of 333 nm when excited at 290 nm that was predominantly due to its two tryptophan residues. The intensity of the emission spectrum of 20α-HSD is only 60 % of that of 3α-HSD, a related HSD which contains three tryptophan residues. The incremental addition of NADPH quenched the fluorescence emission signal and this was accompanied by the formation of an energy-transfer band at 450 nm. Plots of ΔF against [NADP(H)] were fitted to a saturation absorption isotherm, yielding K_d values of 0.36 μM for $NADP^+$ and 0.64 μM for NADPH. The quenching of the protein fluorescence by NADPH in the two enzymes was different. At saturation, NADPH quenched more of the protein fluorescence in 3α-HSD and generated an energy-transfer band of higher intensity than when 20α-HSD was used. Binding testosterone into the 3α-HSD · NADPH binary complex eliminated the energy-transfer band but adding either testosterone or 20α-OHP to the 20α-HSD · NADPH binary complex did not produce this effect.

Inhibition studies

Studies with rat 3α-HSD have shown that commonly used non-steroidal anti-inflammatory drugs (NSAIDs) and steroidal anti-inflammatory drugs (SAIDs) are potent inhibitors of this enzyme [23]. To investigate the effect of these compounds on 20α-HSD activity, their ability to inhibit 20α-OHP oxidation was measured (Table 5). The only NSAID that was a potent competitive inhibitor of 20α-HSD was meclofenamic acid, yielding a K_i of 18.9 μM. In contrast, flufenamic acid, another *N*-phenylanthranilic acid, was a poor inhibitor. In contrast, NSAIDs such as indomethacin (an indoleacetic acid), tolmetin (an *N*-methylpyrroleacetic acid) and SAIDs, which were potent inhibitors of 3α-HSD, had no effect on 20α-HSD activity.

In an attempt to understand the structural basis of HSD inhibition, we also tested non-steroidal oestrogens (hexoestrol, dienoestrol and diethylstilboestrol), the oestrogen antagonist tamoxifen and the phyto-oestrogen genistein. We also included two aldose reductase inhibitors (ARIs), ponalrestat and zopolrestat, in this survey. The synthetic non-steroidal oestrogens inhibited 20α-HSD; hexoestrol was the most potent competitive inhibitor, yielding a K_i of 14.3 μM (Figure 4 and Table 5). Tamoxifen had no inhibitory effect on either 20α-HSD or 3α-HSD. Genistein potently inhibited 3α-HSD but had no effect on 20α-HSD. ARIs were not potent inhibitors of either 20α or 3α-HSDs, although they inhibit aldose reductase with nanomolar affinity [24].

DISCUSSION

Progesterone, produced by the corpus luteum, is essential in all mammals for implantation and the maintenance of early pregnancy [25]. Conversion of progesterone to 20α-OHP by 20α-HSD terminates the action of the hormone, so inhibition of this ovarian enzyme would be useful in maintaining pregnancy. However, ovarian 20α-HSD has been difficult to obtain in large quantities. The native rat ovarian 20α-HSD has been isolated from rat ovarian tissue and was used to study its kinetic mechanism and the stereochemistry of hydride transfer. Like other AKRs, it catalyses an ordered Bi Bi reaction with 4-*pro-R* hydride transfer. However, the published protocols for obtaining native and recombinant enzyme have been unsatisfactory [14–16,26]. Without an expression system with which to produce large quantities of homogeneous recombinant protein, studies on the structure and function and the crystallography of this important enzyme cannot be undertaken. Purification of recombinant 20α-HSD has been attempted previously but the yields were low and the enzyme had less than 20 % of the activity of the native enzyme [16]. Our present studies show that recombinant 20α-HSD can be purified in large quantities with activities towards physiological and non-physiological substrates that are comparable to those exhibited by native enzyme. Because of its simplicity and high yield of 20α-HSD, this purification protocol can be used routinely.

Our kinetic studies have confirmed that purified 20α-HSD displays rigid positional and stereochemistry in that it will oxidize only 20α-hydroxysteroids and reduce 20-oxosteroids with NADP(H) as cofactor. Unlike other HSDs of the AKR superfamily that can use either NAD(H) or NADP(H) as cofactors, 20α-HSD is NADP(H)-specific. From crystallographic information and sequence alignments it is known that all the residues involved in cofactor binding are strictly conserved in HSDs of this superfamily [12]. However, we also know from site-directed mutagenesis and stopped-flow fluorescence experiments on 3α-HSD, a dual-pyridine-nucleotide-specific AKR, that different

Table 5 Inhibition constants (K_i) and pattern of inhibition of recombinant 20α-HSD

The K_i values were determined by measuring the inhibition of 20α-OHP oxidation. Abbreviations: n.i., no inhibition detected at the concentration of inhibitor used; C: competitive inhibition; NC: non-competitive inhibition. Data obtained from refs. *[23] and †[31].

		K_i (μM)	
Inhibitor group	Inhibitor	20α-HSD	3α-HSD
NSAIDs	Meclofenamic acid	18.9 (C)	1.1 μM (C)*
	Flufenamic acid	152 (C)	IC_{50} = 8.52 μM†
	Indomethacin	n.i., [I] > 90 μM	1.1 μM (C)*
	Tolemetin	n.i., [I] > 90 μM	29 μM (C)*
	Ibuprofen	n.i., [I] > 900 μM	37 μM (C)*
	Acetylsalicylic acid	n.i., [I] > 1 mM	650 μM (NC)*
	Salicylic acid	n.i., [I] > 1 mM	115 μM (NC)*
	Acetaminophen	n.i., [I] > 1 mM	2300 μM (NC)*
SAIDs	Betamethasone	n.i., [I] > 30 μM	4.5 μM (NC)*
	Prednisolone	n.i., [I] > 30 μM	17.5 μM (C)*
	6α-Methylprednisolone	n.i., [I] > 30 μM	7.5 μM (C)*
	Prednisone	n.i., [I] > 30 μM	17.5 μM (C)*
ARIs	Ponalrestat	189	IC_{50} = 59 μM†
	Zopolrestat	116	IC_{50} = 46.3 μM†
Anti-oestrogen	Tamoxifen	n.i., [I] > 50 μM	No inhibition
Synthetic oestrogens	Hexoestrol	14.3 (C)	IV_{50} = 4.73 μM*
	Dienoestrol	19.2 (C)	IC_{50} = 19.9 μM
	DES	36.2 (C)	IC_{50} = 158 μM
Phyto-oestrogen	Genistein	$IC_{50} \simeq$ 80 μM	IC_{50} = 6.0 μM

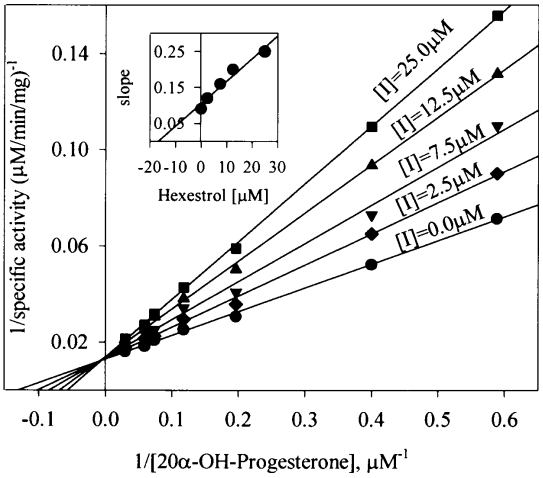

Figure 4 Competitive inhibition of 20α-OHP by the biphenolic synthetic oestrogen hexoestrol

The initial velocity of 20α-OHP oxidation was measured in a 1 ml system in which the concentration of substrate was kept constant (1.7–37 μM) while the concentration of inhibitor was varied from 0 to 25 μM. Each assay contained 2.3 mM $NADP^+$ and 0.8 μg of enzyme. The inset shows a secondary plot in which the slope of the double-reciprocal plot is plotted versus inhibitor concentration.

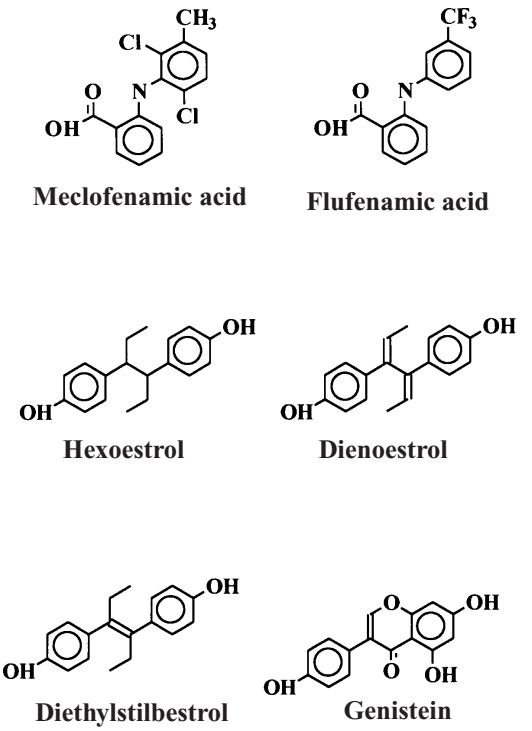

Figure 5 Structures of the two classes of compounds that inhibit 20α-HSD

modes of binding exist for NAD(H) and for NADP(H) (H. Ma, K. Ratnam and T. M. Penning, unpublished work). Until we understand the structural basis for these different modes of binding, we are unable to speculate further on why 20α-HSD is NADP(H)-specific.

Pregnanes other than progesterone have important physiological functions; for example the neuroactive steroid 3α-hydroxy-5α-pregnan-20-one acts as an allosteric effector on the $GABA_A$ receptor (for γ-aminobutyric acid) in the central nervous system and increases Cl^- conductance to exert its anxiolytic and anaesthetic actions [27,28]. Our kinetic studies showed that rat ovarian 20α-HSD can reduce this steroid with high catalytic efficiency, raising the possibility that 20α-HSD isoforms might exist in the central nervous system that serve a similar function.

20α-HSD was also found to reduce the substrates of C_{20-17}-lyase, 17α-hydroxyprogesterone (17α-OHP) and 17α-hydroxypregnenolone [29,30]. C_{20-17}-lyase is an important enzyme in determining whether C_{21} or C_{19} steroids are produced in the adrenal and gonads. The reaction is particularly important in the adrenal because 17α-hydroxypregnenolone and 17α-OHP either are converted to glucocorticoids or undergo the subsequent lyase reaction to form dehydroepiandrosterone and androstenedione respectively. Both 17α-hydroxylase and C_{20-17}-lyase reactions are catalysed by the same enzyme, raising the issue of what determines the reaction pathway. It is unknown whether adrenal or gonadal 20α-HSD isoforms exist that can reduce 17α-hydroxyprogesterone and 17α-hydroxypregnenolone and thus deprive the lyase of its substrates.

We also examined the fluorescence properties of 20α-HSD for the first time. Quenching of the intrinsic tryptophan fluorescence of AKRs on the binding of NADP(H) has been used to determine the K_d values of cofactors [31]. Our quenching studies showed that 20α-HSD has a high affinity for $NADP^+$ and NADPH, with K_d values of 0.36 and 0.64 μM respectively. By comparing the fluorescence properties of 20α-HSD with 3α-HSD [31], several important differences were noted. First, the intensity of the emission spectrum for 20α-HSD at its λ_{max} is only 60% of that of 3α-HSD and is blue-shifted to 333 nm (the λ_{max} of 3α-HSD is 336 nm). The findings are consistent with the fact that 20α-HSD contains only two of the three tryptophan residues (Trp-86 and Trp-148) present in 3α-HSD, and one of these must be more exposed to solvent to explain the blue-shift. Secondly, binding of

NADPH quenched the protein fluorescence spectrum and generated an energy-transfer band in both enzymes with a λ_{max} of 450 nm. However, NADPH quenched much more protein fluorescence and generated an energy-transfer band of much higher intensity in 3α-HSD than in 20α-HSD. Because the interactions between Trp-86 and the 1,4-dihydronicotinamide ring of the cofactor are responsible for the energy transfer [31], this interaction must be disrupted in 20α-HSD. Thirdly, the binding of testosterone to the 3α-HSD·NADPH complex attenuated the energy-transfer band, suggesting that the A-ring of testosterone was inserted between Trp-86 and the cofactor in the resultant ternary complex, a fact confirmed by the crystal structure of the 3α-HSD·$NADP^+$·testosterone complex [32]. However, neither testosterone nor 20α-OHP had the same effect on the 20α-HSD·NADPH binary complex.

Previous studies have shown that bovine testicular 20α-HSD is identical with aldose reductase [33,34], whereas aldose reductase from human brain and aldehyde reductase from human liver have been shown to reduce C_{21} steroid aldehydes such as isocorticosteroids [35]. This raises the issue that aldose and aldehyde reductase inhibitors might effect the metabolism of C_{21} steroids; this is an important consideration for inhibitor design. To examine inhibitor specificity, we tested NSAIDs and SAIDs, which are known inhibitors of 3α-HSD [23], and ARIs that have been used for clinical trials, as well as the synthetic oestrogen hexoestrol, the phyto-oestrogen genistein and the anti-oestrogen tamoxifen. Many of these compounds were potent inhibitors of 3α-HSD but had no affect on 20α-HSD activity. Only meclofenamic acid and the synthetic non-steroidal oestrogens potently inhibited 20α-HSD. 20α-HSD and 3α-HSD share high sequence identity and are predicted to share the same $(\alpha/\beta)_8$ motif present in the 3α-HSD crystal structure [32]. Despite this similarity, the substrate-binding site of 20α-HSD can discriminate between different 3α-HSD inhibitors.

By comparing the structures of these inhibitors we found that only compounds with two aromatic rings inhibited 20α-HSD and they belonged to two chemical classes (Figure 5). The first class was the *N*-phenylanthranilates, e.g. meclofenamic acid and flufenamic acid, which are NSAIDs. NSAIDs usually contain a carboxylic acid linked to an aniline (*N*-phenylanthranilate), an indole (indomethacin) or a pyrrole (*N*-pyrroleacetic acid). Although previous modelling studies showed that indomethacin and the 3α-hydroxysteroid androsterone were structurally related [36], indomethacin inhibited only 3α-HSD activity, not 20α-HSD activity. The introduction of functional groups into *N*-phenylanthranilates had a profound effect on inhibitory potency. Thus the presence of a bis-halide in meclofenamic acid increased inhibitory potency 8-fold over flufenamic acid, which lacks these groups. The second class is the biphenolic non-steroidal oestrogens, e.g. hexoestrol, dienoestrol, diethylstilboestrol and genistein. These compounds have hydroxy groups at the equivalent of the C-3 and the C-17 positions of steroids; however, the rigidity of the compounds had an important role in determining inhibitory potency. Thus the most rigid compound, genistein, had no inhibitory effect towards 20α-HSD and the most flexible compound, hexoestrol, was the most potent inhibitor. Importantly, both indomethacin and genistein were very potent inhibitors of 3α-HSD, suggesting that the inhibitor-binding modes of 20α-HSD and 3α-HSD are quite different. These inhibition studies suggest that selective non-steroidal inhibitors could be developed for ovarian 20α-HSD that could be useful in maintaining pregnancy.

Received 28 January 1999/26 April 1999; accepted 24 May 1999

We thank Dr. Chien-Fu Hung for technical support, and Dr. Jane M. Vanderkooi for the use of the spectrofluorimeters in her laboratory. This work was supported by NIH grant DK47015 to T.M.P.; H.M. was partly supported by an NIH Predoctoral Training Grant in Pharmacology.

REFERENCES

1 Wiest, W. G. and Wilcox, R. B. (1961) J. Biol. Chem. **236**, 2425–2428
2 Wiest, W. G. and Forbes, T. R. (1964) Endocrinology (Baltimore) **74**, 149–152
3 Wiest, W. G., Kidwell, W. R. and Balogh, Jr., K. (1968) Endocrinology (Baltimore) **82**, 844–859
4 Diaz-Zagoya, J. C., Wiest, W. G. and Arias, F. (1979) Am. J. Obstet. Gynecol. **133**, 673–676
5 Diaz-Zagoya, J. C., Wiest, W. G. and Arias, F. (1979) Am. J. Obstet. Gynecol. **135**, 809–813
6 Tanaka, N. M., Shiota, K., Noda, K., Kadosawa, T., Mochizuki, M., Nishimura, R., Takahashi, M. and Sasaki, N. (1996) J. Vet. Med. Sci. **58**, 623–627
7 Valavaara, R. (1997) Oncology **11**, 14–18
8 Horwitz, K. B., Wei, L. L., Sedlacek, S. M. and d'Arville, C. N. (1985) Recent Prog. Horm. Res. **41**, 249–316
9 Mao, J., Duan, W. R., Albarracin, C. T., Parmer, T. G. and Gibori, G. (1994) Biochem. Biophys. Res. Commun. **201**, 1289–1295
10 Miura, R., Shiota, K., Noda, K., Yagi, S., Ogawa, T. and Takahashi, M. (1994) Biochem. J. **299**, 561–567
11 Zhong, L., Barkai, U., Mao, J. F., Frasor, J. and Gibori, G. (1998) Biochem. Biophys. Res. Commun. **249**, 797–803
12 Jez, J. M., Bennett, M. J., Schlegel, B. P., Lewis, M. and Penning, T. M. (1997) Biochem. J. **326**, 625–635
13 Jez, J. M., Flynn, T. G. and Penning, T. M. (1997) Biochem. Pharmacol. **54**, 639–647
14 Pongsawasdi, P. and Anderson, B. M. (1984) Biochim. Biophys. Acta **799**, 51–58
15 Noda, K., Shiota, K. and Takahashi, M. (1991) Biochim. Biophys. Acta **1079**, 112–118
16 Mao, J., Duan, W. R., Zhong, L., Gibori, G. and Azhar, S. (1997) Endocrinology (Baltimore) **138**, 182–190
17 Lowry, O. H., Rosebrough, N. J., Farr, A. L. and Randall, R. J. (1951) J. Biol. Chem. **193**, 265–275
18 Wilkinson, G. N. (1961) Biochem. J. **80**, 324–332
19 Leatherbarrow, R. J. (1987) ENZFITTER: A Non-Linear Regression Data Analysis Program for the IBM PC (and true compatibles), BioSoft, Cambridge, UK
20 Segel, I. H. (1975) in Enzyme Kinetics, 2nd edn., pp. 101–160, Wiley, New York
21 Penning, T. M. and Sharp, R. B. (1987) Biochem. Biophys. Res. Commun. **148**, 646–652
22 Wintergalen, N., Thole, H. H., Galla, H.-J. and Schlegel, W. (1995) Eur. J. Biochem. **234**, 264–270
23 Penning, T. M., Mukharji, I., Barrows, S. and Talalay, P. (1984) Biochem. J. **222**, 601–611
24 Wilson, D. K., Tarle, I., Petrash, J. M. and Quiocho, F. A. (1993) Proc. Natl. Acad. Sci. U.S.A. **90**, 9847–9851
25 Hoyer, P. B. (1998) J. Soc. Gynecol. Invest. **5**, 49–57
26 Mori, M. and Wiest, W. G. (1979) J. Steroid Biochem. **11**, 1443–1449
27 Majewska, M. D., Harrison, N. L., Schwartz, R. D., Barker, J. L. and Paul, S. M. (1986) Science **232**, 1004–1007
28 Smith, S. S., Gong, Q. H., Hsu, F.-C., Markowitz, R. S., ffrench-Mullen, J. M. and Li, X. (1998) Nature (London) **392**, 926–930
29 Nakajin, S. and Hall, P. F. (1981) J. Biol. Chem. **256**, 3871–3876
30 Miller, W. L., Auchus, R. J. and Geller, D. H. (1997) Steroids **62**, 133–142
31 Jez, J. M., Schlegel, B. P. and Penning, T. M. (1996) J. Biol. Chem. **271**, 30190–30198
32 Bennett, M. J., Albert, R. H., Jez, J. M., Ma, H., Penning, T. M. and Lewis, M. (1997) Structure **5**, 799–812
33 Warren, J. C., Murdock, G. L., Ma, Y., Goodman, S. R. and Zimmer, W. E. (1993) Biochemistry **32**, 1401–1406
34 Petrash, J. M., Harter, T. M. and Murdock, G. L. (1997) Adv. Exp. Med. Biol. **414**, 465–473
35 Wermuth, B. and Monder, C. (1983) Eur. J. Biochem. **131**, 423–426
36 Penning, T. M. and Talalay, P. (1983) Proc. Natl. Acad. Sci. U.S.A. **80**, 4504–4508
37 Pawlowski, J. E. and Penning, T. M. (1994) J. Biol. Chem. **269**, 13502–13510